

# High-Mobility Organic Thin Film Transistors Based on Benzothiadiazole-Sandwiched Dihexylquaterthiophenes

Prashant Sonar,<sup>†,‡</sup> Samarendra P. Singh,<sup>†,‡</sup> Sundarraj Sudhakar,<sup>‡,§</sup> Ananth Dodabalapur,<sup>\*,‡,||</sup> and Alan Sellinger<sup>\*,‡</sup>

*Institute of Materials Research and Engineering (IMRE) and the Agency for Science, Technology and Research (A\*STAR), 3 Research Link, Singapore 117602, Republic of Singapore, and Microelectronics Research Center, The University of Texas at Austin, Austin, Texas 78758, USA*

Received January 14, 2008

We report here the synthesis, characterization, and organic thin-film transistor (OTFT) mobilities of 4,7-bis(5-(5-hexylthiophen-2-yl)thiophen-2-yl)benzo[1,2,5]thiadiazole (**DH-BTZ-4T**). **DH-BTZ-4T** was prepared in one high-yield step from commercially available materials using Suzuki chemistry and purified by column chromatography. OTFTs with hole mobilities of 0.17 cm<sup>2</sup>/(Vs) and on/off current ratios of 1 × 10<sup>5</sup> were prepared from **DH-BTZ-4T** active layers deposited by vacuum deposition. As **DH-BTZ-4T** is soluble in common solvents, solution processed devices were also prepared by spin coating yielding preliminary mobilities of 6.0 × 10<sup>-3</sup> cm<sup>2</sup>/(Vs). The promising mobilities and low band gap (1.90 eV) coupled with solution processability and ambient stability makes this material an excellent candidate for application in organic electronics.

## 1. Introduction

New semiconducting organic materials are being developed in many laboratories with a view to improve key performance metrics such as mobility and to alter physical properties such as the energy gap and energy levels.<sup>1–6</sup> Devices and systems made with such materials are expected to find use in several applications such as flexible display backplanes, light-emitting devices, sensors of various kinds, etc. One class of materials that shows promise is based on benzothiadiazoles. Many reports have appeared on the use of 2,1,3-benzothiadiazole (BTZ) based materials for various applications such as organic light emitting diodes (OLEDs),<sup>7–9</sup> field effect transistors (OTFTs)<sup>10–13</sup> and photovoltaic cells.<sup>14–19</sup>

The ease of producing BTZ-based materials with well-defined molecular structures and high purity renders them promising candidates as charge transporting and light emitting materials in thin-film optoelectronic devices such as organic light emitting transistors (OLETs).<sup>11</sup> This interest results from BTZ having a high electron affinity combined with facile synthesis and functionalization properties.<sup>20,21</sup> For example, the introduction of thiophene groups on both sides of the BTZ molecule results in donor–acceptor–donor (D–A–D) heterocyclic materials with low band gap properties.<sup>22–24</sup> The Donor–Acceptor (D–A) approach has been demonstrated and applied with success in the case of polymers to achieve low band gap conjugated materials whereas there are relatively few reports about the analogous

\* Corresponding author. E-mail: ananth@mer.utexas.edu (A.D.); alan-sellinger@imre.a-star.edu.sg (A.S.). Tel: (512) 232-1890(A.D.); 65-6874-4153(A.S.). Fax: (512) 471-8575 (A.D.); 65-6872-7528 (A.S.).

<sup>†</sup> These authors contributed equally to this work.

<sup>‡</sup> Institute of Materials Research and Engineering (IMRE) and the Agency for Science, Technology and Research (A\*STAR).

<sup>§</sup> Present Address: BASF South East Asia Pte Ltd., Competence Center for Nanostructured Surfaces, No. 61, Science Park Road, #03-01 The Galen, Singapore Science Park III, Singapore 117525.

<sup>||</sup> The University of Texas at Austin.

- (1) Dimitrakopoulos, C. D.; Malenfant, P. R. L. *Adv. Mater.* **2002**, *14*, 99.
- (2) Horowitz, G. *J. Mater. Res.* **2004**, *19*, 1946.
- (3) Anthony, J. *Chem. Rev.* **2006**, *106*, 5028.
- (4) Facchetti, A.; Mushrush, M.; Katz, H. E.; Marks, T. J. *Adv. Mater.* **2003**, *15*, 33.
- (5) Jones, B. A.; Ahrens, M. J.; Yoon, M. H.; Facchetti, A.; Marks, T. J.; Wasielewski, M. R. *Angew. Chem., Int. Ed.* **2004**, *43*, 6363.
- (6) Katz, H. E.; Bao, Z. N.; Gilat, S. L. *Acc. Chem. Res.* **2001**, *34*, 359.
- (7) Ritonga, M. T. S.; Sakurai, H.; Hirao, T. *Tetrahedron Lett.* **2002**, *43*, 9009.
- (8) Neto, B. A. D.; Lopes, A. S. A.; Ebeling, G.; Goncalves, R. S.; Costa, V. E. U.; Quina, F. H.; Dupont, J. *Tetrahedron* **2005**, *46*, 10975.
- (9) Yamashita, Y.; Suzuki, K.; Tomura, M. *Synth. Met.* **2003**, *133*, 341.
- (10) Akhtaruzzaman, M.; Kamata, N.; Nishida, J.; Ando, S.; Tada, H.; Tomura, M.; Yamashita, Y. *Chem. Commun.* **2005**, *25*, 3183.
- (11) Kono, T.; Kumaki, D.; Nishida, J.; Sakanoue, T.; Motoyasu, K.; Tada, H.; Tokito, S.; Yamashita, Y. *Chem. Mater.* **2007**, *6*, 1218.

- (12) Zhang, M.; Tsao, H. N.; Pisula, W.; Yang, C. D.; Mishra, A. K.; Mullen, K. *J. Am. Chem. Soc.* **2007**, *129*, 3472.
- (13) Zaumseil, J.; Donley, C. L.; Kim, J. S.; Friend, R. H.; Siringhaus, H. *Adv. Mater.* **2006**, *20*, 2708.
- (14) Huang, J.; Xu, Y.; Hou, Q.; Yang, W.; Yuan, M.; Cao, Y. *Macromol. Rapid Commun.* **2002**, *23*, 709.
- (15) Svensson, M.; Zhang, F.; Veenstra, S. C.; Verhees, W. J. H.; Hummelen, J. C.; Kroon, J. M.; Inganäs, O.; Andersson, M. R. *Adv. Mater.* **2003**, *12*, 988.
- (16) Bundgaard, E.; Krebs, F. C. *Sol. Energy Mater. Sol. Cells.* **2007**, *11*, 1019.
- (17) Bundgaard, E.; Krebs, F. C. *Polym. Bull.* **2005**, *3*, 157.
- (18) Mühlbacher, D.; Scharber, M.; Morana, M.; Zhu, Z. G.; Waller, D.; Gaudiana, R.; Brabec, C. *Adv. Mater.* **2006**, *18*, 2884.
- (19) Blouin, N.; Michaud, A.; Leclerc, M. *Adv. Mater.* **2007**, *19*, 2295.
- (20) Akhtaruzzaman, M.; Tomura, M.; Nishida, J.; Yamashita, Y. *J. Org. Chem.* **2004**, *69*, 2953.
- (21) Kato, S.; Matsumoto, T.; Ishi-i, T.; Thiemann, T.; Shigeiwa, M.; Gorohamaru, H.; Maeda, S.; Yamashita, Y.; Mataka, S. *Chem. Commun.* **2004**, *69*, 2432.
- (22) Jayakannan, M.; Hal, P. A. Van.; Janssen, R. A. J. *J. Polym. Sci. Part A: Polym. Chem.* **2001**, *40*, 251.
- (23) Mullekom, H. A. M. van.; Venkema, J. A. J. M.; Meijer, E. W. *Chem.—Eur. J.* **1998**, *4*, 1235.
- (24) Park, Y. S.; Kim, D.; Hoosung, L.; Moon, B. *Org. Lett.* **2006**, *8*, 4702.

small molecules and oligomers.<sup>25–27</sup> Furthermore, low band gap materials with a lowest unoccupied molecular orbital (LUMO) ( $\geq -3.2$  eV) are desired in order to achieve environmentally stable organic semiconductors.<sup>28</sup> The strong intermolecular interaction in such oligomers may lead to molecular packing with a large electronic bandwidth and consequently high charge carrier mobility for OTFT applications.<sup>8</sup> D–A–D based oligomers are interesting semiconducting molecules not only for the understanding of band gap engineering but also for the study of charge transport mechanisms in such molecular systems. It has also been reported that D–A–D systems show strong intermolecular interaction leading to high lattice energy.<sup>24</sup> As a result, D–A–D systems may also exhibit interactions that may generate highly ordered crystalline film and consequently enhanced charge transport capability. Furthermore, long aliphatic chains at both ends of the D–A–D rodlike systems may help induce liquid crystalline properties.

In this paper, we report the synthesis and characterization of a new benzothiadiazole sandwiched dihexylquaterthiophene organic semiconductor (**DH-BTZ-4T**) and its use as the active semiconductor in p-channel OTFTs from both vacuum deposition and solution processable methods.

## 2. Experimental Section

**General Description.** All commercially available materials were used as received unless otherwise noted. All reactions were carried out using Schlenk techniques in an argon or nitrogen atmosphere with anhydrous solvents.

**Instruments.** <sup>1</sup>H and <sup>13</sup>C NMR data were performed on a Bruker DPX 400 MHz spectrometer with chemical shifts referenced to residual CHCl<sub>3</sub> in CDCl<sub>3</sub>. Matrix assisted laser desorption/ionization time-of-flight (MALDI-TOF) mass spectra were obtained on a Bruker Autoflex TOF/TOF instrument using dithranol as the matrix. Differential scanning calorimetry (DSC) was carried out under nitrogen on a TA Instrument DSC Q100 instrument (scanning rate of 10 °C min<sup>-1</sup>). Thermal gravimetric analysis (TGA) was carried out using a TA Instrument TGA Q500 instrument (heating rate of 10 °C min<sup>-1</sup>). Cyclic voltammetry experiments were performed using an Autolab potentiostat (model PGSTAT30) by Echochimie. All CV measurements were recorded in dichloromethane with 0.1 M tetrabutylammonium hexafluorophosphate as supporting electrolyte (scan rate of 100 mV s<sup>-1</sup>). The experiments were performed at room temperature under an argon blanket with a conventional three electrode configuration consisting of a platinum wire working electrode, a gold counter electrode, and an Ag/AgCl in 3 M KCl reference electrode. UV–vis spectra were recorded on a Shimadzu model 2501-PC. Photoluminescence (PL) spectra were measured on a Perkin-Elmer (LS50B) spectrofluorimeter.

The photomicrographs of the **DH-BTZ-4T** were taken using a Nikon OPTIPHOT2-POL polarizing optical microscope fitted with a hot stage using a temperature programmer TP-93 and a TMC-6 RGB 1/2" color CCD camera with net 500X magnification. The sample was placed on a glass slide, covered with a glass coverslip and heated on the hot stage at 10 °C/min and cooled at 5 °C/min. All the images have a scale bar of 50 μm.

**Synthesis of DH-BTZ-4T.** 4,7-Dibromo-2,1,3-benzothiadiazole (1.00 g, 3.33 mmol), 2-(5-(5-hexylthiophen-2-yl)thiophen-2-yl)-4,4,5,5-tetramethyl dioxaborolane (3.20 g, 8.50 mmol, 2.5 equiv.), and tetrakis(triphenylphosphine) Pd(0) (78 mg, 0.06 mmol) were added to a 100 mL Schlenk flask and subjected to three vacuum/argon refill cycles. Toluene (20 mL) and a nitrogen degassed aqueous solution of 2 M K<sub>2</sub>CO<sub>3</sub> (8 mL, 16.0 mmol) were added and stirred for 10 min under argon. The mixture was heated at 80 °C for 24 h and monitored via thin layer chromatography (TLC) for reaction completion. Toluene was removed using a rotovap and the product was extracted with dichloromethane, successively washed with water, and dried over MgSO<sub>4</sub>. Removal of the solvent afforded the crude product as brown oil, which was then precipitated out in methanol. The crude product was purified using column chromatography (silica gel, hexane:dichloromethane as eluent) to yield 1.10 g (52%) of the product as a deep red crystalline solid. <sup>1</sup>H NMR (CDCl<sub>3</sub>): δ 0.90 (t, 6H, 2CH<sub>3</sub>), 1.33 (m, 12H, 6CH<sub>2</sub>), 1.70 (q, 4H, 2CH<sub>2</sub>), 2.80 (t, 4H, 2CH<sub>2</sub>), 6.72 (s, 2H, Th), 7.10–7.18 (d, 4H, Th), 7.81 (s, 2H, Th), 8.02 (s, 2H, Btz). <sup>13</sup>C NMR (CDCl<sub>3</sub>): δ 14.39, 22.93, 29.14, 30.62, 31.94, 124.18, 125.31, 125.44, 125.93, 128.65, 135.06, 137.89, 139.78, 146.43, 152.92. MALDI-TOF-MS (dithranol) *m/z*: 632.24; calcd for C<sub>34</sub>H<sub>36</sub>N<sub>2</sub>S<sub>5</sub> = 632.15. Anal. Calcd for C<sub>34</sub>H<sub>36</sub>N<sub>2</sub>S<sub>5</sub>: C, 64.51; H, 5.73; N, 4.43; S, 25.33. Found: C, 64.81; H, 5.92; N, 4.76; S, 25.25.

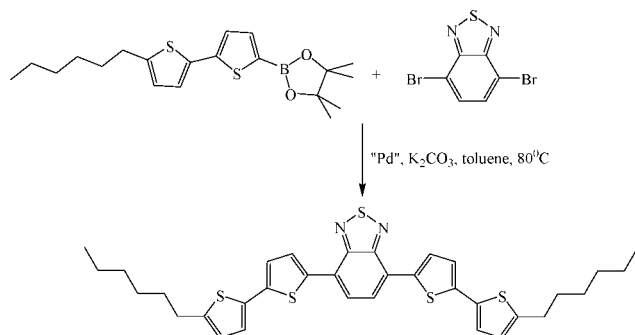
**OTFT Fabrication and Characterization.** Top contact organic thin film transistors (OTFTs) were fabricated on heavily doped n<sup>+</sup>-Si wafers with 200 nm of thermally grown SiO<sub>2</sub>. In order to investigate the effect of substrate temperature during deposition on device performance, a series of OTFTs were fabricated at room temperature, 50 °C, and 80 °C. The effect of surface modifications on device performances using hexamethyldisilazane (HMDS) and octyltrichlorosilane (OTS) self-assembled monolayers (SAMs) on Si/SiO<sub>2</sub> were also studied. HMDS treatments were carried out by exposing the Si/SiO<sub>2</sub> wafers to HMDS at room temperature under nitrogen overnight.<sup>29</sup> OTS treated substrates were obtained by immersing Si/SiO<sub>2</sub> substrates in 0.1 M OTS solutions in toluene at 60 °C for 20 min, and subsequently rinsed by toluene and isopropanol.<sup>30</sup> For all sets of OTFTs, a 35 nm film of **DH-BTZ-4T** was deposited using vacuum sublimation at a rate of 0.5–1.0 Å/s under a pressure of  $\sim 7 \times 10^{-6}$  mbar. Alternatively, thin films of **DH-BTZ-4T** were spun cast from solution using 12 mg/mL solutions in chloroform, and spin speeds of 1200 rpm for 60 s. Patterned gold layers of thicknesses  $\sim 100$  nm were deposited for source (S) and drain (D) electrodes through a shadow mask. For a typical OTFT device reported here, the S–D channel length (*L*) and channel width (*W*) was 100 μm and 3 mm, respectively. The device characteristics of the OTFTs were measured at room temperature under nitrogen with a Keithley 4200 parameter analyzer. The field effect mobility ( $\mu$ ) was calculated from the transfer characteristics in the saturation regime ( $V_d \approx -70$  V) and current  $I_{ON}/I_{OFF}$  ratio was calculated from the  $I_{ds}$  at  $V_{gs} = 0$  V and  $V_{gs} = -70$  V.

**XRD and AFM images.** X-ray diffraction patterns of **DH-4T BTZ** thin films deposited at room temperature, 50 °C, and 80 °C on the Si/SiO<sub>2</sub> substrates were obtained with a PANalytical X'PERT PRO system using Cu K $\alpha$  source in air. AFM images were obtained with a molecular Imaging Veeco Metrology Digital Instruments microscope in air.

(25) Havinga, E. E.; Hoeve, W.; Wynberg, H. *Polym. Bull.* **1992**, *29*, 119.  
(26) Havinga, E. E.; Hoeve, W.; Wynberg, H. *Synth. Met.* **1993**, *55–57*, 299.  
(27) Tanaka, S.; Yamashita, Y. *Synth. Met.* **1997**, *84*, 229.  
(28) Zaumseil, J.; Sirringhaus, H. *Chem. Rev.* **2007**, *107*, 296.

(29) Yoon, M. H.; Dibeneditto, S. A.; Facchetti, A.; Marks, T. J. *J. Am. Chem. Soc.* **2005**, *127*, 1348.  
(30) Ong, B. S.; Wu, Y.; Liu, P.; Gardener, S. *Adv. Mater.* **2005**, *17*, 1141.

## Scheme 1. Synthesis of DH-BTZ-4T



## 3. Result and Discussion

The structure of the **DH-BTZ-4T** is similar to that of dihexylquaterthiophene (**DH-4T**), a widely studied semiconductor for p-channel OFETs.<sup>31</sup> With the addition of the BTZ unit between the two hexylbithiophene units, it was anticipated that the band gap and HOMO level compared to dihexylquaterthiophene (**DH-4T**) would be strategically altered (lower band gap and HOMO level further from vacuum level) to provide a molecule with high mobility, red emission, and increased ambient stability for potential application in organic light emitting transistors (OLETs).<sup>32</sup>

**DH-BTZ-4T** was prepared in a one step Suzuki coupling reaction using commercially available 5'-hexyl-2,2'-bithiophene-5-boronic acid pinacol ester and 4,7-dibromobenzothiazole with 2 M  $K_2CO_3$  and  $Pd(PPh_3)_4$  in refluxing toluene (see Scheme 1). An excess of the boronic acid pinacol ester derivative was used to ensure completion of the coupling reaction. The crude compound was purified by gradient column chromatography from pure hexane to hexane:dichloromethane (90:10  $\rightarrow$  80:20) to yield a readily soluble deep red colored solid in >50% yield. The synthesis of this molecule was scaled up to the 1.0 g scale with comparable isolated yields. The compound **DH-BTZ-4T** was soluble in common organic solvents such as toluene, chloroform and THF with maximum attainable concentrations of 12–15 mg mL<sup>-1</sup>. The molecular weight and purity of the **DH-BTZ-4T** was confirmed by MALDI-TOF analysis and is shown in Figure 1. The purity of **DH-BTZ-4T** was further confirmed by elemental analysis and <sup>1</sup>H and <sup>13</sup>C NMR spectroscopy (Figure S1).

The UV/vis absorption spectrum of **DH-BTZ-4T** in chloroform shows two distinct peaks at 366 and 521 nm, as compared to just a single peak for **DH-4T** (absorption maxima  $\sim$ 380 nm).<sup>33</sup> The additional peak at 521 nm results from the introduction of the BTZ moiety. The **DH-BTZ-4T** exhibits a strong red emission maxima at 650 nm (see Figure 2) which is largely red-shifted ( $\sim$ 145 nm) compared to the emission maxima of **DH-4T**.<sup>33</sup>

Thermogravimetric analysis (TGA) showed the thermal decomposition temperature ( $T_d$ , 5 wt % loss) around 400 °C (Figure 3a) which indicates the high thermal stability of the compound for vacuum sublimation processing. The thermal

behavior of the **DH-BTZ-4T** was determined by a repeated heating and cooling cycle using differential scanning calorimetry (DSC). This measurement showed multiple endothermic peaks at 125, 175, 202, and 210 °C indicative of liquid crystalline behavior (Figure 3b). Liquid crystalline behavior was also confirmed by using hot-stage polarized optical microscopy (POM) which clearly indicates the crystalline to liquid crystalline (LC) transition at 175 °C and LC-to-isotropic transition at 210 °C (Figure 4). LC behavior has been shown to be a favorable property for predicting materials with good charge transport mobilities.<sup>34</sup>

The electrochemical stability of **DH-BTZ-4T** was investigated by cyclic voltammetry (CV). The CV showed reversible oxidation and reduction peaks at 0.92 and  $-1.35$  V, respectively (Figure 5) from which we estimate an ionization potential (IP, HOMO level) of 5.15 eV ( $IP = E_{ox}^{onset} + 4.4$ ) and an electron affinity (EA, LUMO level) of 3.25 eV ( $EA = E_{red}^{onset} + 4.4$ ).<sup>35,36</sup> The HOMO level indicates that the material is oxidatively stable in air—a key requirement for organic electronic applications. For example, working transistors could be realized after heating the material in air for several minutes at 185 °C. The band gap of the molecule calculated from CV measurements (HOMO–LUMO) of 1.90 eV matches quite well with the optical band gap derived from the UV absorption onset (1.95 eV). The observed reversible oxidation and reduction peaks can be attributed to the hexylbithiophene (donor) and benzothiazole (acceptor) portions of the molecule respectively. The alternating electron D–A arrangement causes an interaction of the highest occupied molecular orbital (HOMO) of the donor and the lowest unoccupied molecular orbital (LUMO) of the acceptor resulting in a reduced band gap in these materials.<sup>37,38</sup>

To investigate the crystalline properties of **DH-BTZ-4T**, X-ray diffraction (XRD) experiments in reflection mode were performed on thin films deposited on Si/SiO<sub>2</sub> substrates at RT, 50 °C, and 80 °C (Figure 6a). The increasing intensity of the reflection peak at 2.56 °2 $\theta$  as a function of substrate temperature indicates the progressively higher order. Furthermore, the additional reflection peak at 3.45 degrees 2 $\theta$  ( $d_{spacing}$  of 25.6 Å) for films deposited at 80 °C shows the enhanced crystalline nature of the thin films with increasing substrate temperature. The peak at 2.56° 2 $\theta$  ( $d_{spacing}$  of 34.5 Å), is consistent with the molecular length of **DH-BTZ-4T**, which is estimated to be 34.0 Å, shown in Figure 6b. The second order reflection peak at 6.93 degrees 2 $\theta$ , as shown in the inset of Figure 6, further shows the high crystalline nature of the thin films. Taking into account the estimated molecular length of **DH-BTZ-4T** (34.0 Å) and XRD data, the material seems to have an interdigitated molecular arrangement via strong  $\pi$ – $\pi$  stacking of D–A–D cores and hydrophobic interaction of alkyl side chains, as shown in

(31) Katz, H. E.; Torsi, L.; Dodabalapur, A. *Chem. Mater.* **1995**, *7*, 2235.  
 (32) Zaumseil, J.; Friend, R. H.; Sirringhaus, H. *Nat. Mater.* **2006**, *5*, 69.  
 (33) Lim, E.; Jung, B. J.; Shim, H. K.; Taguchi, T.; Noda, B.; Kambayashi, T.; Mori, T.; Ishikawa, K.; Takezoe, H.; Do, L. M. *Org. Electron.* **2006**, *7*, 121.

(34) Ponomarenko, S.; Kirchmeyer, S. *J. Mater. Chem.* **2003**, *13*, 197.  
 (35) Yang, C. J.; Jenkhe, S. A. *Macromolecules* **1995**, *28*, 1180.  
 (36) Kulkarni, A. P.; Tonzola, C. J.; Babel, A.; Jenkhe, S. A. *Chem. Mater.* **2004**, *16*, 4556.  
 (37) Roncali, J. *Chem. Rev.* **1997**, *97*, 173.  
 (38) Van Mullekom, H. A. M.; Vekemans, J. A. J. M.; Havinga, E. E.; Meijer, E. W. *Mater. Sci. Eng.* **2001**, *32*, 1.

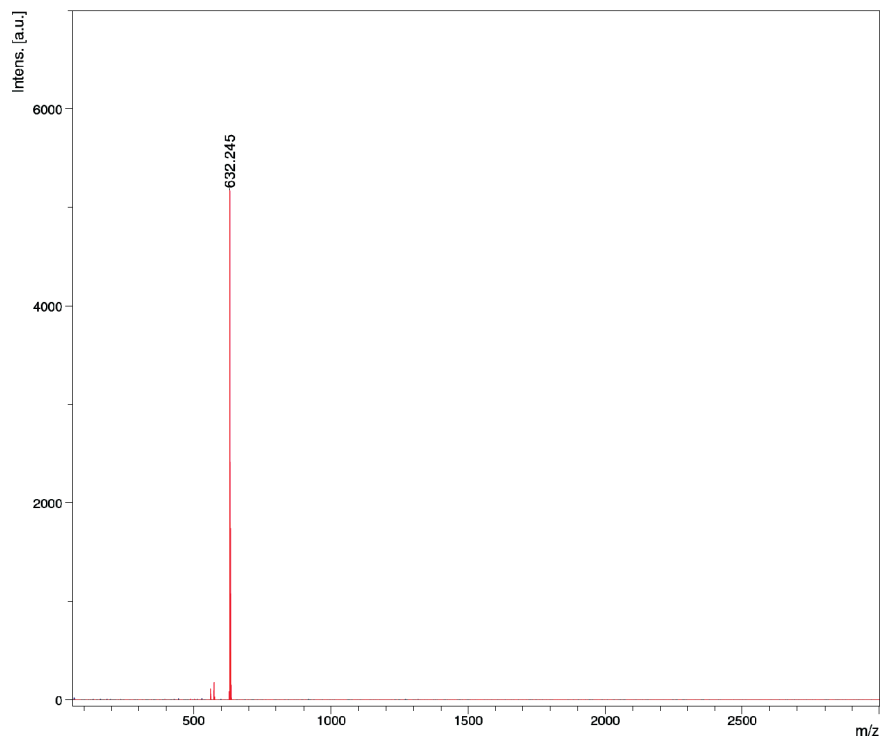


Figure 1. MALDI-TOF spectrum of DH-BTZ-4T.

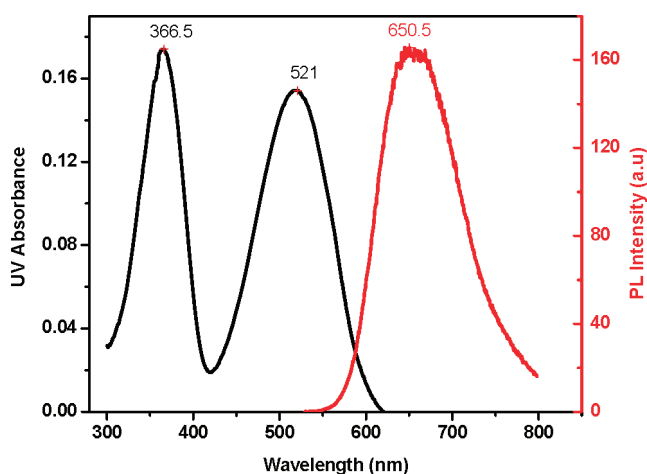


Figure 2. UV-vis absorption (black) and PL spectra (red) of DH-BTZ-4T in  $\text{CHCl}_3$ .

Figure 6b. Such kinds of observations have been previously reported using D-A-D type liquid crystals with pyridazine core.<sup>24</sup>

Atomic force microscopy (AFM) was used in order to investigate the morphology of DH-BTZ-4T thin films deposited at the three temperatures on Si/SiO<sub>2</sub> substrates (Figure 7). As shown, the thin film morphology evolves from a relatively smooth surface at RT to having progressively more rodlike features with large grain sizes at 50° and 80 °C respectively. This result is encouraging as in general, the field-effect mobility for organic semiconductor films depends on the grain size as well as molecular orientation on the substrate.<sup>1,2,39</sup>

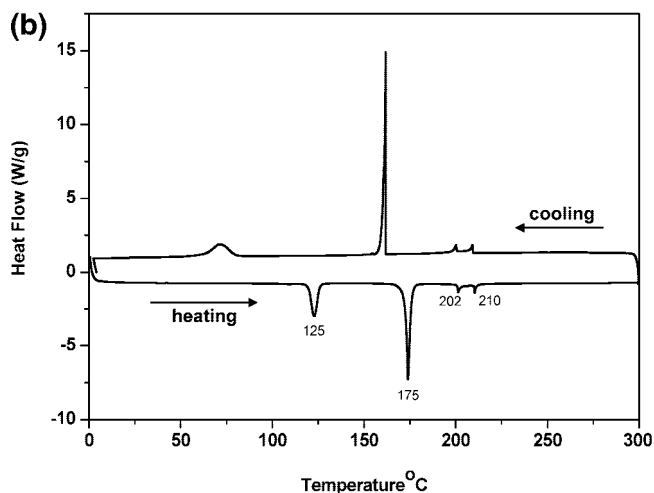
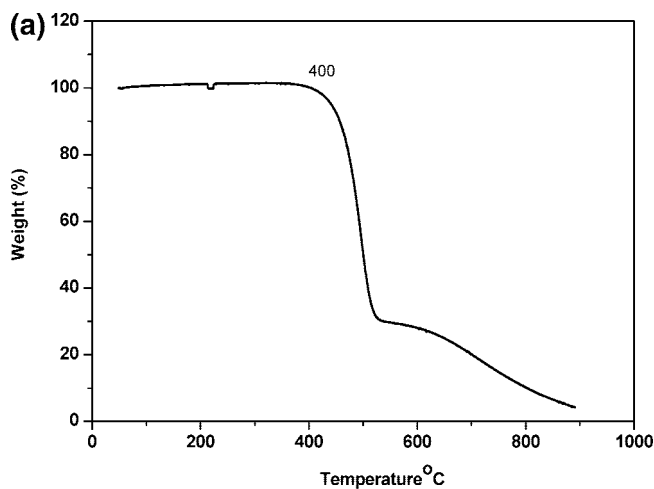
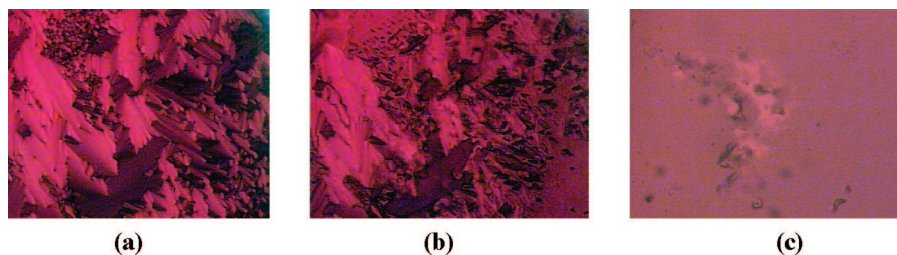
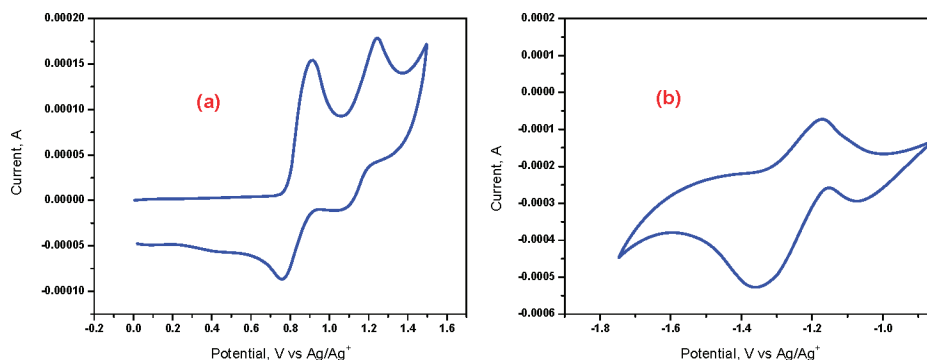


Figure 3. (a) TGA of DH-BTZ-4T showing thermal decomposition temperature (Td) at 400 °C (5% weight loss) indicative of high thermal stability; (b) DSC of DH-BTZ-4T showing multiple transitions, indicative of liquid crystalline properties.

(39) Dimitrakopoulos, C. D.; Mascaro, D. J. *IBM J. Res. Dev.* **2001**, *45*, 11.



**Figure 4.** Polarized optical micrographs of **DH-BTZ-4T** at (a) 185 °C, on heating, (b) 195 °C, on heating, (c) 205 °C, on heating showing liquid crystalline to isotropic transitions.



**Figure 5.** (a) Oxidation and (b) reduction cycles of **DH-BTZ-4T** in 0.1 M TBAPF<sub>6</sub>/CH<sub>2</sub>Cl<sub>2</sub>,  $\nu = 100\text{mVs}^{-1}$ .

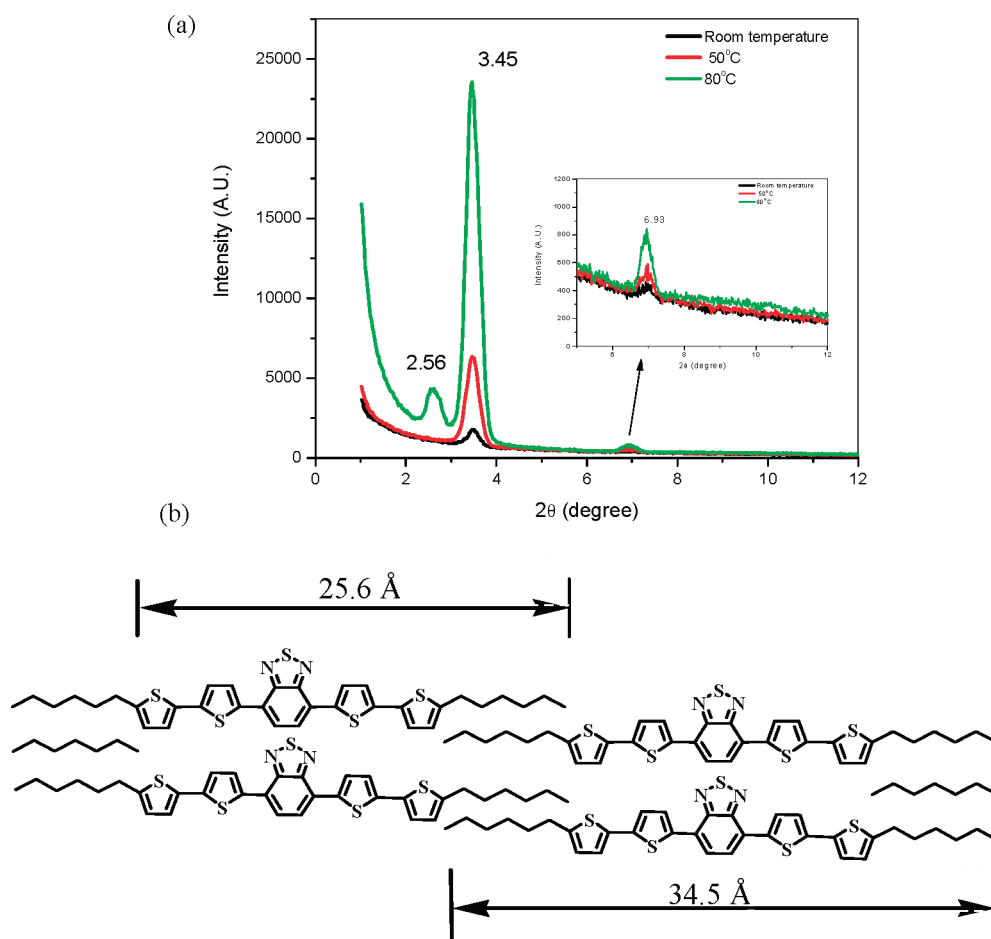


**Figure 6.** (a) X-ray diffraction (XRD) patterns of **DH-BTZ-4T** film on Si/SiO<sub>2</sub> substrate deposited at various temperatures. (b) A proposed molecular arrangement of **DH-BTZ-4T**.

The fabrication of thin film transistors by vacuum deposition and solution processing techniques were next performed.

The effect of surface modification and substrate temperature on device mobilities were examined. The current—voltage

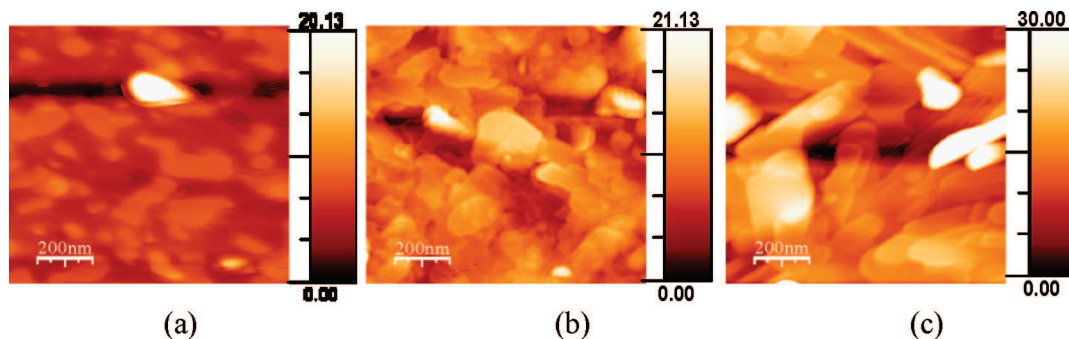


Figure 7. AFM images of DH-BTZ-4T thin films deposited by vacuum sublimation on Si/SiO<sub>2</sub> substrate at (a) room temperature, (b) 50 °C, and (c) 80 °C.

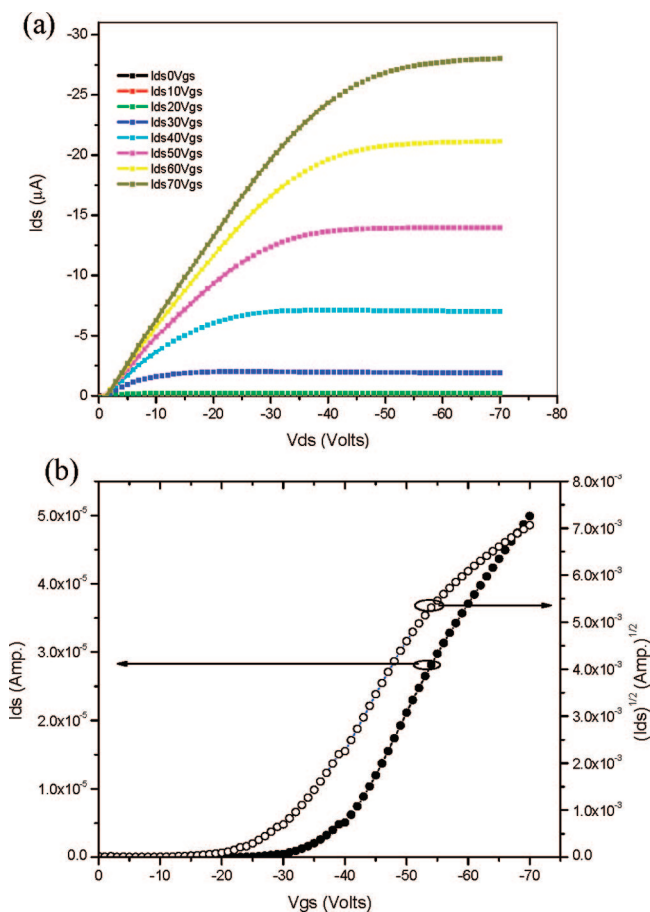


Figure 8. Current-voltage (a)  $I_{ds}$ - $V_{ds}$ , and (b)  $I_{ds}$ - $V_{gs}$ , characteristic of DH-BTZ-4T on OTS treated substrate.

characteristics of the vacuum deposited OTFTs processed at room temperature on OTS treated Si/SiO<sub>2</sub> substrates are shown in Figure 8. The devices exhibit p-channel performance with the highest mobility, calculated from the saturation regime, of 0.17 cm<sup>2</sup>/(V s), an  $I_{ON}/I_{OFF}$  ratio of  $\sim 1 \times 10^5$ , and threshold voltage of -28 V as shown in Table 1. Furthermore, as shown in Table 1 an 8.5 $\times$  and 100 $\times$  enhancement in mobility and on/off ratio respectively were observed from OTS treated SiO<sub>2</sub> surfaces prior to DH-BTZ-4T deposition. Solution processed devices have shown mobility of  $6.0 \times 10^{-3}$  cm<sup>2</sup>/(V s) for OTS treated substrates processed at room temperature with an  $I_{ON}/I_{OFF}$  ratio of  $\sim 1 \times 10^4$  as shown in Table 1. Furthermore, the solution processed devices have shown remarkably low

Table 1. Device Performance of Evaporation- and Solution-Processed OTFTs on Bare and SAM-Modified Si/SiO<sub>2</sub> Substrates

no.	surface treatment (SAM)	evaporation-processed		solution-processed	
		$\mu$ (cm <sup>2</sup> /(V s))	$I_{ON}/I_{OFF}$	$\mu$ (cm <sup>2</sup> /(V s))	$I_{ON}/I_{OFF}$
1	bare Si/SiO <sub>2</sub>	0.02	$\sim 1 \times 10^3$	0.004	$\sim 1 \times 10^4$
2	HMDS	0.06	$\sim 1 \times 10^4$	0.006	$\sim 1 \times 10^4$
3	OTS	0.17	$\sim 1 \times 10^5$	0.006	$\sim 1 \times 10^4$

Table 2. Device Performance of OTFTs Processed at Different Substrate Temperatures

no.	substrate $T$ (°C)	$\mu$ (cm <sup>2</sup> /(V s))	$I_{ON}/I_{OFF}$
1	room temperature	0.02	$\sim 1 \times 10^3$
2	50	0.04	$\sim 1 \times 10^3$
3	80	0.07	$\sim 1 \times 10^4$

threshold voltages of <7 V. Work to optimize the performance of solution processed devices using different processing conditions is underway. Table 2 shows the effects of substrate temperature on OTFT performance of OTFTs on Si/SiO<sub>2</sub> surfaces. For example, we observed a 3.5 $\times$  and 10 $\times$  enhancement in mobility and on/off ratio respectively when depositing on a substrate heated at 80 °C versus room temperature. Note that the vacuum sublimed thin film transistors have shown better charge transport property compared to solution processed devices due to enhanced quality and homogeneity of the films. Such a difference is quite common in small molecule and oligomer systems that have been both vacuum sublimed and solution cast.<sup>1</sup> All the device results reported here are highly reproducible.

#### 4. Conclusions

We have developed a benzothiadiazole sandwiched oligothiophene based D-A-D molecule, DH-BTZ-4T, using a simple one step Suzuki coupling reaction. This material shows liquid crystalline behavior, is soluble in common solvents, and shows significant red shifts in absorption and emission properties as compared to the more commonly studied and related dihexylquaterthiophene (DH-4T). Furthermore, DH-BTZ-4T has shown very promising performance as a p-channel OTFT with a mobility of 0.17 cm<sup>2</sup>/(V s) for vacuum-deposited thin films on OTS treated substrates at room temperature. DH-BTZ-4T is also soluble in common solvents and shows a mobility of  $6.0 \times 10^{-3}$  cm<sup>2</sup>/(V s) for preliminary devices

prepared via spin coating onto OTS treated devices. Studies on various processing conditions to further increase mobilities are currently under progress.

**Acknowledgment.** The authors acknowledge the Institute of Materials Research and Engineering (IMRE) and the Visiting Investigatorship Programme (VIP) of the Agency for Science, Technology and Research (A\*STAR), Republic of Singapore, for financial support. We thank Mr. Lawrence

Dunn for valuable discussions, and Mr. Teck Lip Tam and Mr. Poh Chong Lim for help in characterization and XRD experiments respectively.

**Supporting Information Available:**  $^1\text{H}$  and  $^{13}\text{C}$  NMR spectra for **DH-BTZ-4T** (PDF). This material is available free of charge via the Internet at <http://pubs.acs.org>.

CM800139Q